A&A 652, A102 (2021)
https://doi.org/10.1051/0004-6361/202140608

Astronomy & Astrophysics

Evolution of the local spiral structure of the Milky Way revealed by open clusters⋆

C. J. Hao[1,2], Y. Xu[1,2], L. G. Hou[3], S. B. Bian[1,2], J. J. Li[1], Z. Y. Wu[3,4], Z. H. He[1,2], Y. J. Li[1], and D. J. Liu[1,5]

[1] Purple Mountain Observatory, Chinese Academy of Sciences, Nanjing 210023, PR China
e-mail: xuye@pmo.ac.cn
[2] School of Astronomy and Space Science, University of Science and Technology of China, Hefei 230026, PR China
[3] National Astronomical Observatories, Chinese Academy of Sciences, 20A Datun Road, Chaoyang District, Beijing 100101, PR China
[4] School of Astronomy and Space Science, University of Chinese Academy of Sciences, Beijing 101408, PR China
[5] College of Science, China Three Gorges University, Yichang 443002, PR China

Received 19 February 2021 / Accepted 27 June 2021

ABSTRACT

The structure and evolution of the spiral arms of our Milky Way are basic but long-standing questions in astronomy. In particular, the lifetime of spiral arms is still a puzzle and has not been well constrained from observations. In this work, we aim to inspect these issues using a large catalogue of open clusters. We compiled a catalogue of 3794 open clusters based on *Gaia* EDR3. A majority of these clusters have accurately determined parallaxes, proper motions, and radial velocities. The age parameters for these open clusters are collected from references or calculated in this work. In order to understand the nearby spiral structure and its evolution, we analysed the distributions, kinematic properties, vertical distributions, and regressed properties of subsamples of open clusters. We find evidence that the nearby spiral arms are compatible with a long-lived spiral pattern and might have remained approximately stable for the past 80 million years. In particular, the Local Arm, where our Sun is currently located, is also suggested to be long-lived in nature and probably a major arm segment of the Milky Way. The evolutionary characteristics of nearby spiral arms show that the dynamic spiral mechanism might be not prevalent for our Galaxy. Instead, density wave theory is more consistent with the observational properties of open clusters.

Key words. Galaxy: evolution – Galaxy: structure – Galaxy: kinematics and dynamics – open clusters and associations: general

1. Introduction

Accurately revealing the spiral structure of the Milky Way and its evolution has attracted the attention of many astronomers. After the M 33 galaxy was explored by Hubble (1926), it was speculated that our Milky Way is also possibly a spiral galaxy. Since then, much effort has been dedicated to uncover the spiral structure of the Galaxy with different kinds of tracers and methods (e.g., Lindblad 1927; Oort et al. 1958; Becker 1963, 1964; Becker & Fenkart 1970; Georgelin & Georgelin 1976; Moffat et al. 1979; Russeil 2003; Paladini et al. 2004; Dias & Lépine 2005; Xu et al. 2006, 2018a, 2021; Moitinho et al. 2006; Vázquez et al. 2008; Reid et al. 2009, 2019; Moitinho 2010; Hou & Han 2014, 2015; Poggio et al. 2021). However, because the Sun is deeply embedded in the Galactic disc, multiple structures at different distances along the line of sight are superimposed; this makes very difficult to accurately decompose these structures and depict the actual spiral structure (Xu et al. 2018b). Moreover, another big challenge is reliably tracing the Galaxy's morphology to the past to ultimately understand its evolutionary history.

Open clusters (OCs) are one of the good spiral tracers and have some specific advantages for understanding the properties of spiral structure of the Galaxy. An open cluster is a group of stars that formed from the same giant molecular cloud, which are roughly the same age. Unlike the other good tracers for investigating the spiral arms of the Galaxy (e.g., high-mass star formation region (HMSFR) masers, massive O−B type (OB) stars, and HII regions), the ages of OCs cover a wide range, from a few million years (Myr) to tens of billions of years, making them potentially good tracers for investigating the spiral structure outlined by young to old objects, and in particular the evolution of spiral arms. In addition, the large number of cluster members makes it possible to derive more accurate values of cluster parameters (e.g., distances, proper motions, and radial velocities) than those of individual star. The spiral structure of the Galaxy has been explored by many research works using OCs as tracers.

The relationship between OCs and spiral arms was first discussed by Becker (1963, 1964), who studied a sample of 156 OCs with photometric distances at that time. Becker suggested that the distribution of those OCs with earliest spectral type of O−B2 followed three spiral arm segments in the solar neighbourhood. In comparison, the distribution of older OCs with earliest spectral type from B3 to F did not present arm-like structures and seemed to be random. These results were confirmed by Becker & Fenkart (1970) and Fenkart & Binggeli (1979) with larger samples of OCs. While a diferent explanation was proposed by Janes & Adler (1982) and Lynga (1982), these authors suggested that the distributions of OCs seemed more like some clumpy-like concentrations or complexes rather than a spiral

⋆ The catalogue is only available at the CDS via anonymous ftp to cdsarc.u-strasbg.fr (130.79.128.5) or via http://cdsarc.u-strasbg.fr/viz-bin/cat/J/A+A/652/A102

pattern. Dias & Lépine (2005) used a sample of 212 OCs to showed that the young OCs (ages $< 1.2 \times 10^7$ yr) still remain in the three major arm segments in the solar neighbourhood, that is, the Perseus, Local, and Sagittarius-Carina Arms. The OCs ~20 Myr in age are leaving the spiral arms and moving to the inter-arm regions, while for the older OCs, their distributions do not present clear clump-like or spiral-like structures. Dias & Lépine (2005) also estimated the spiral pattern rotation speed of the Milky Way with OCs and confirmed that a dominant fraction of the OCs are formed in spiral arms. These results were recently updated by Dias et al. (2019) with the second data release of *Gaia* (Gaia Collaboration 2018). Moitinho et al. (2006) analysed the stellar photometry data for many OCs; a sample of 61 OCs was used to trace the disc structure in the third Galactic quadrant. The detailed spiral structure in the third Galactic quadrant was also explored by Vázquez et al. (2008) by taking advantage of the data of young OCs, blue plumes, and molecular clouds. For a review about the previous efforts to use OCs to study the Galactic structure, we recommend Moitinho (2010). Later, Camargo et al. (2013) studied a sample of young OCs, which are related with the Perseus Arm and even the Outer Arm (also see Bobylev & Bajkova 2014). By taking advantage of the second data release of *Gaia*, Cantat-Gaudin et al. (2018, 2019, 2020) have derived the members and mean parameters for more than 1800 Galactic OCs. The projected distribution of these OCs onto the Galactic disc was compared with a spiral arm model of our Galaxy (Reid et al. 2014).

In brief, it is commonly accepted that young OCs can be used to trace the nearby spiral arms, while older OCs have more scattered distribution, which may be used to represent the distribution of older stellar components in the Galactic disc. However, the evolutionary properties and the lifetime of the spiral arms of the Galaxy are still puzzles and have not been well constrained from observations. With its specialty, OC serves as good tracer for better understanding these issues. Fortunately, the number of OCs and the accuracy of OC parameters (parallaxes, proper motions, and radial velocities) have been improved significantly in the past few years, largely as a result of the efforts of *Gaia* (see Table 1). In this work, we aim to compile a large catalogue of OCs from references and accurately derive their parallax distances, proper motions, and radial velocities from the latest *Gaia* Early Data Release 3 (hereafter *Gaia* EDR3) (Gaia Collaboration 2016, 2021). This largest catalogue of OCs available to date provides a good chance to study the above issues about spiral structure of the Galaxy, not only to map the nearby spiral arms, but also to understand their evolution, and further, to place observational constraints on the different evolutionary mechanisms.

This article is organised as follows. In Sect. 2, we describe the sample of OCs compiled in this work. The results and discussions are presented in Sect. 3, including the spiral structure in the solar neighbourhood traced by OCs, the kinematic properties of OCs, the evolutionary properties of their scale heights, and a regression analysis. Conclusions are given in Sect. 4.

2. Sample

To better understand the spiral structure of the Galaxy with OCs, an updated OC catalogue with accurately measured parameters from *Gaia* EDR3 is necessary. The recently published *Gaia* EDR3 contains the positions, parallaxes, and proper motions for more than 1.5 billion stars of different types, ages, and evolutionary stages in the whole sky (Gaia Collaboration 2021). For the sources with magnitude $G < 15$, the parallax uncertainties could be 0.02−0.03 mas, and the proper motion uncertainties could be 0.02−0.03 mas yr^{-1}. *Gaia* EDR3 provides excellent database to improve the parameter accuracies for a large number of OCs.

Table 1. References for the previously known OCs.

Reference	OCs number	Data used
Dias et al. (2002)	2167	WEBDA [(1)] et al.
Dias et al. (2014)	1805	UCAC4 [(2)]
Kharchenko et al. (2013)	3006	2MASS [(3)] and PPMXL [(4)]
Schmeja et al. (2014)	139	2MASS
Scholz et al. (2015)	63	PPMXL and UCAC4
Cantat-Gaudin et al. (2018)	1229	*Gaia* DR2
Cantat-Gaudin et al. (2019)	41	*Gaia* DR2
Castro-Ginard et al. (2018)	23	*Gaia* DR2 and TGAS [(5)]
Castro-Ginard et al. (2019)	53	*Gaia* DR2
Castro-Ginard et al. (2020)	582	*Gaia* DR2
Liu & Pang (2019)	76	*Gaia* DR2
He et al. (2021)	74	*Gaia* DR2
Ferreira et al. (2020)	25	*Gaia* DR2

Notes. [(1)] WEBDA: `http://obswww.unige.ch/webda/`; [(2)] UCAC = United States Naval Observatory CCD Astrograph Catalog; [(3)] 2MASS = Two Micron All Sky Survey; [(4)] PPMXL: `https://dc.zah.uni-heidelberg.de/ppmxl/q/cone/info`; [(5)] TGAS = *Tycho-Gaia* Astrometric Solution.

Up to now, thousands of OCs have been identified, but scattered in references. Dias et al. (2002) assembled a large catalogue of OCs based on many previous studies, which contains 2167 objects. Dias et al. (2014) gave the proper motions and membership probabilities for 1805 optically visible OCs. By taking advantage of near-infrared photometric data of approximately 470 million objects in Two Micron All Sky Survey (2MASS, Skrutskie 2006) and proper motions from the PPMXL catalogue (Roeser et al. 2010), Kharchenko et al. (2013) completed a survey of all previously known OCs called the Milky Way Star Clusters Catalog (MWSC), which lists 3006 objects, including known OCs and candidates, globular clusters, associations, and asterisms. Subsequently, the MWSC catalogue was complemented by 139 new OCs at high Galactic latitudes (Schmeja et al. 2014) and 63 new OCs identified by Scholz et al. (2015). After the publication of *Gaia* DR2 (Gaia Collaboration 2018), the membership probabilities of ~1200 OCs presented in previous catalogues were recalculated by Cantat-Gaudin et al. (2018). These authors also discovered 60 new OCs. Besides, the radial velocities of 861 OCs in Cantat-Gaudin et al. (2018) were obtained by Soubiran et al. (2018). Castro-Ginard et al. (2018) developed a machine-learning approach and found 23 new OCs from *Gaia* DR2. Soon after, Castro-Ginard et al. (2019) detected 53 new OCs in the direction of the Galactic anti-centre. Cantat-Gaudin et al. (2019) identified 41 new OCs in the direction of the Perseus Arm. Meanwhile, 76 new OCs were reported by Liu & Pang (2019). Recently, 582 new OCs were discovered by Castro-Ginard et al. (2020), 25 new OCs were detected by Ferreira et al. (2020), and 74 new OCs were found by He et al. (2021), respectively.

As the first step of this work, we compiled a large catalogue, which includes 3794 Galactic OCs collected from references (see Table 1). The procedure is described as follows. Firstly, 2469 OCs were selected from Kharchenko et al. (2013), which provides details of member stars for each of the OCs. Then, the

member stars with probabilities greater than 60% were picked out to conduct positional cross-matching with *Gaia* EDR3 using a matching radius of 1 arcsec. Making use of the sample-based clustering search method (Hao et al. 2020), which was an adaptation of the OC search method presented in Castro-Ginard et al. (2018), we yielded 2457 OCs. For the OC catalogue of Dias et al. (2002), we cross-matched it with the catalogue of Kharchenko et al. (2013), and 315 OCs not listed in Kharchenko et al. (2013) were obtained. The sample-based clustering search method was applied to these targets, and we got 309 OCs. Subsequently, we cross-matched the catalogue of Cantat-Gaudin et al. (2018) with these 2766 OCs and then obtained 153 OCs. For these 153 OCs, only the member stars with probabilities greater than 60% were picked out. The same procedure was conducted on the catalogue of Cantat-Gaudin et al. (2019). Then, we obtained detailed parameters of 658 OCs from the catalogues of Castro-Ginard et al. (2018, 2019, 2020), including the member stars. In addition, we collected 76 new OCs from the catalogue of Liu & Pang (2019), 25 new OCs from Ferreira et al. (2020), and 74 new OCs from He et al. (2021), respectively. Finally, we obtained a total of 3794 OCs. The parameters of these OCs were determined using *Gaia* EDR3.

Gaia EDR3 provides parallax uncertainties for almost all of its stars. To obtain precise parallax for each of these OCs, we only extracted the member stars whose parallax uncertainties are smaller than 10%. Not all of the 3794 OCs have member stars with parallax uncertainties better than 10%. Hence, a high-accuracy subsample of 3611 OCs was extracted, in which, 1742 OCs have radial velocities. For these 1742 OCs, the means, standard errors, and uncertainties of their radial velocities were determined using the method of Soubiran et al. (2018). After that, the member stars brighter than $G = 17$ mag were used to determine the position and proper motions for each of these OCs. For the bright member stars, the uncertainties are better than 0.05 mas for the position and 0.07 mas yr^{-1} for the proper motions, respectively (Gaia Collaboration 2021). In terms of photometry, for the stars of $G = 17$ mag, the associated photometric error is 0.001 mag and 0.012 mag for $G_{\rm BP}$, and 0.006 mag for $G_{\rm RP}$ (Gaia Collaboration 2021). The determined parameters of the OCs, together with the reference(s) where the OC was selected, all are given in the on-line catalogue of this work.

Some recent works (e.g., Cantat-Gaudin et al. 2018; Cantat-Gaudin & Anders 2020; Monteiro et al. 2020) suggest that there are some false positive or non-existing clusters in the previous catalogues. Most of these controversial or erroneous objects are the alleged old and high-altitude clusters (Cantat-Gaudin & Anders 2020). We checked the 146 false positive or nonexistent clusters given by Dias et al. (2002), and we found that 81 of these are not included in our catalogue. In this work, our aim is to study the spiral arms in the Galactic disc, and we primarily adopt relatively young OCs (e.g., ages < 100 Myr). For the 65 possibly false positive clusters suggested by Dias et al. (2002) and kept in our compiled catalogue, only 16 of these are <100 Myr in age. In comparison, the total number of OCs <100 Myr in age in our catalogue is 1229. Hence, we believe that this problem does not influence the following analysis results about the spiral structure of the Galaxy. Besides, the ages for the 2837 OCs in our compiled catalogue were already given in previous works; these are adopted directly. For the remaining 957 (~25%) OCs, most of these (~70%) are recently identified OCs based on the *Gaia* data. We determined their ages and the errors following the methods described in Liu & Pang (2019), Hao et al. (2020), and He et al. (2021). The age parameter for each of the 3794 OCs and the corresponding reference(s) are also given in the on-line catalogue.

3. Results and discussions

3.1. Spiral structure in the solar neighbourhood

Figure 1 presents the projected distributions of OCs onto the Galactic disc. Figure 1a shows that the 633 young OCs (YOCs; i.e., ages < 20 Myr) in our catalogue are concentrated in distinct structures, which are almost concordant with the known spiral arms outlined by HMSFR masers (Reid et al. 2019) and/or bright OB stars (Xu et al. 2018a, 2021). A large number of YOCs are located in the Perseus, Local, Sagittarius–Carina, and Scutum–Centaurus Arms, which seem to be the nurseries for many OCs. These arm features traced by YOCs extend as far as ~3 to 8 kpc along different spiral arms. These properties are in general consistent with previous results (e.g., see Becker & Fenkart 1970; Dias & Lépine 2005; Moitinho et al. 2006; Vázquez et al. 2008; Dias et al. 2019; Cantat-Gaudin et al. 2018, 2020). In Fig. 1a, it is also shown that the more populous OCs (i.e., those with more member stars) seem to be more concentrated on the major spiral arms than the less populous ones. In addition, spur-like features indicated by the concentration of some YOCs are visible in the inter-arm regions, which is consistent with the results shown using HMSFR masers (Reid et al. 2019) and bright OB stars (Xu et al. 2018a, 2021). This all suggests that our Milky Way is not a pure grand-design spiral, but perhaps a multi-armed spiral galaxy showing complex substructures (Xu et al. 2016).

The distributions of older OCs are shown in Figs. 1b–d. Consistent with previous results (e.g., Moitinho et al. 2006; Vázquez et al. 2008; Bobylev & Bajkova 2014; Reddy et al. 2016; Dias & Lépine 2005; Cantat-Gaudin et al. 2018, 2020), the OCs are gradually dispersed in the Galactic disc as they age. Structural features are still discernible for the populous OCs with ages of tens of million years, but the older OCs (e.g., ages > 200 Myr) present more diffuse distributions. Indeed, when using the OCs older than 1000 Myr as tracers, spiral arm features are almost unrecognisable. These properties indicate that as the YOCs age they gradually migrate away from their birthplaces, probably accompanied by the evolution of spiral arms.

Inspired by the above phenomena, we considered that as OCs gradually age the spiral arms traced by OCs of different ages are probably not the same; instead, they can be used to reflect the evolution of the spiral arms of the Galaxy. A subsample of OCs below 100 Myr in age is extracted from our catalogue and used to explore this issue. To ensure that there are plenty of OCs in each age interval, we divide those OCs that are below 100 Myr into three different age groups of <20 Myr (633 clusters), 20−60 Myr (334 clusters), and 60−100 Myr (262 clusters). From their distributions, the three nearby spiral arms (i.e., the Sagittarius-Carina, Local, and Perseus Arms) are discernible. For the more distant Scutum–Centaurus Arm, as fewer OCs are located in it, this arm cannot be well traced and hence is omitted in the following analysis. Then, in order to make a comparison with the maser results, we determine the parameters of spiral arms with the same method of Reid et al. (2019), which is used in analysing their maser parallax data. To fit the pitch angle and arm width for a spiral arm traced by YOCs, a logarithmic spiral-arm model is adopted (Reid et al. 2014),

$$\ln(R/R_{\rm ref}) = -(\beta - \beta_{\rm ref}) \tan\varphi, \quad (1)$$

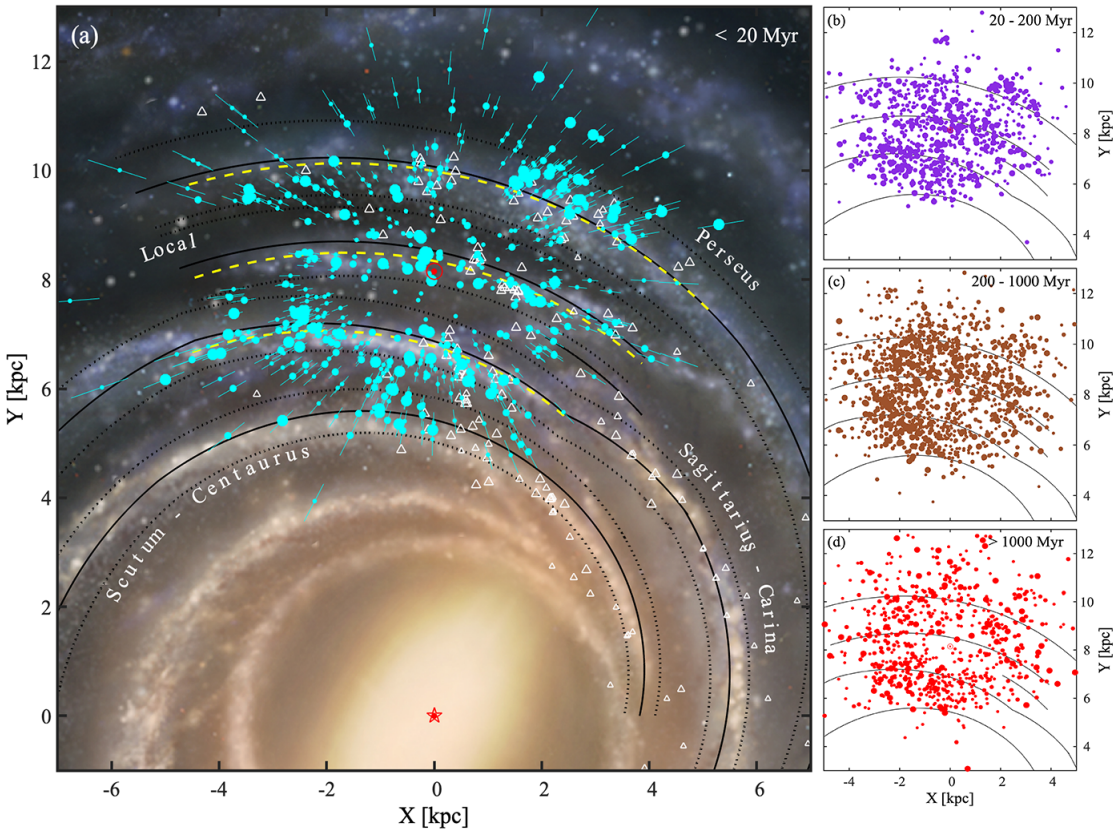

Fig. 1. Distributions of Galactic OCs. (*a*) YOCs (cyan dots; ages < 20 Myr) and HMSFR masers (white triangles) projected onto the Galactic disc. The dot size is proportional to the number of cluster members. The solid curved lines trace the centres (and dotted lines the widths enclosing 90% of the masers) of the best-fit spiral arms given by Reid et al. (2019). The distance uncertainties of the masers are indicated by the inverse size of the symbols. The yellow dashed lines denote the best-fit spiral arm centres from the distribution of YOCs. The Galactic centre (red star) is at (0,0) kpc and the Sun (red symbol) is at (0, 8.15) kpc. The background is a new concept map of the Milky Way credited by Xing-Wu Zheng & Mark Reid BeSSeL/NJU/CFA. The distributions of the older clusters are shown in *panels b–d* for the OCs with ages of 20−200 Myr (purple dots), 200−1000 Myr (brown dots), and >1000 Myr (red dots), respectively. The dot size is also proportional to the number of cluster members. The parallax uncertainties of the OCs shown are all smaller than 10%.

where $R_{\rm ref}$ is the reference Galactocentric radius, $\beta_{\rm ref}$ is the reference azimuthal angle, and φ is the pitch angle. The zero point of the Galactocentric azimuthal angle, β, is defined as a line towards the Sun from the Galactic centre, and the azimuthal angle increases towards the direction of Galactic rotation. The quantity R is the Galactocentric radius at a Galactocentric azimuth β. The fitting results are listed in Table 2.

In comparison to the values derived by using HMSFR masers, the pitch angles of the three nearby spiral arms traced by OCs tend to be smaller; the differences become larger when older OCs were used as tracers, thus implying a tighter winding of the spiral arms traced by older OCs. This is possibly a true feature for the Milky Way; however, the differences of pitch angles are not significant when considering the fitting uncertainties and higher quality data of OCs would be necessary to confirm this. Besides, arm width is also an important parameter for a spiral arm. We note that the fitted arm widths for the OCs with ages of 60−100 Myr are inclined to be larger than those of the HMSFR masers. In comparison, the arm widths derived from YOCs are in general consistent with HMSFR masers.

3.2. Kinematic properties of OCs

With the distances, proper motions, and radial velocities for the 1742 OCs in the high-accuracy sample, we can derive their three-dimensional (3D) velocity information following the methods of Xu et al. (2013) and Reid et al. (2019). The 3D velocities were straightforwardly calculated using the linear speeds projected onto the celestial sphere and radial velocities, which were obtained from the proper motions and distances. Then, the peculiar motions (PMs; i.e., non-circular motions) of the OCs were estimated by subtracting the effect of Galactic rotation and the solar PMs using the updated Galactic parameters. In this approach, we adopted a Galactic rotation speed of $236 \pm 7\,{\rm km\,s^{-1}}$, where the Sun is at a distance of 8.15 ± 0.15 kpc to the Galactic centre (Reid et al. 2019). Solar PMs of $U_\odot = 10.6 \pm 1.2\,{\rm km\,s^{-1}}$, $V_\odot = 10.7 \pm 6.0\,{\rm km\,s^{-1}}$, and $W_\odot = 7.6 \pm 0.7\,{\rm km\,s^{-1}}$ were assumed (Reid et al. 2019), which are the velocity components towards the Galactic centre in the direction of Galactic rotation and towards the North Galactic Pole, respectively. The sources with an uncertainties larger than $10\,{\rm km\,s^{-1}}$ were eliminated in the following analysis.

In Fig. 2, we present the PMs of YOCs in the solar neighbourhood. The PMs of YOCs seem to be random. As the gravitational potential of the Galactic bar is weak in these regions, the PMs of YOCs should be intrinsic. We find that the average peculiar motion is $1.3 \pm 0.2\,{\rm km\,s^{-1}}$ towards the Galactic centre and $-6.8 \pm 0.2\,{\rm km\,s^{-1}}$ in the direction of the Galactic rotation. Hence, there is an average lagging motion for YOCs behind the Galactic rotation. Similar properties were recently noticed for HMSFR

Table 2. Best-fit parameters of nearby spiral arms using HMSFR masers and OCs of different age groups.

	Arm	φ (deg)	$R_{\rm ref}$ (kpc)	$\beta_{\rm ref}$ (deg)	Arm width (kpc)
HMSFR masers	Sagittarius-Carina	17.1 ± 1.6	6.04 ± 0.09	24	0.27 ± 0.04
	Local	11.4 ± 1.9	8.26 ± 0.05	9	0.31 ± 0.05
	Perseus	10.3 ± 1.4	8.87 ± 0.13	40	0.35 ± 0.06
YOCs (<20 Myr)	Sagittarius-Carina	16.2 ± 0.4	6.72 ± 0.07	2	0.27 ± 0.02
	Local	10.8 ± 0.6	8.18 ± 0.06	6	0.24 ± 0.06
	Perseus	9.6 ± 0.8	9.42 ± 0.04	20	0.33 ± 0.03
OCs (20–60 Myr)	Sagittarius-Carina	15.7 ± 0.5	6.80 ± 0.07	2	0.30 ± 0.03
	Local	10.7 ± 0.8	8.24 ± 0.07	6	0.31 ± 0.03
	Perseus	9.0 ± 1.0	9.45 ± 0.06	20	0.36 ± 0.04
OCs (60–100 Myr)	Sagittarius-Carina	15.2 ± 0.5	6.79 ± 0.07	2	0.33 ± 0.04
	Local	8.9 ± 0.9	8.09 ± 0.06	5	0.40 ± 0.03
	Perseus	9.0 ± 0.9	9.43 ± 0.07	20	0.39 ± 0.05

Notes. For each spiral arm, the best-fit pitch angle (φ), initial radius ($R_{\rm ref}$), reference Galactocentric azimuth angle ($\beta_{\rm ref}$), and arm width are listed. The OCs are divided into three subsamples: (1) YOCs (<20 Myr, 633 clusters); (2) OCs with ages from 20 to 60 Myr (334 clusters); and (3) OCs with ages from 60 to 100 Myr (262 clusters).

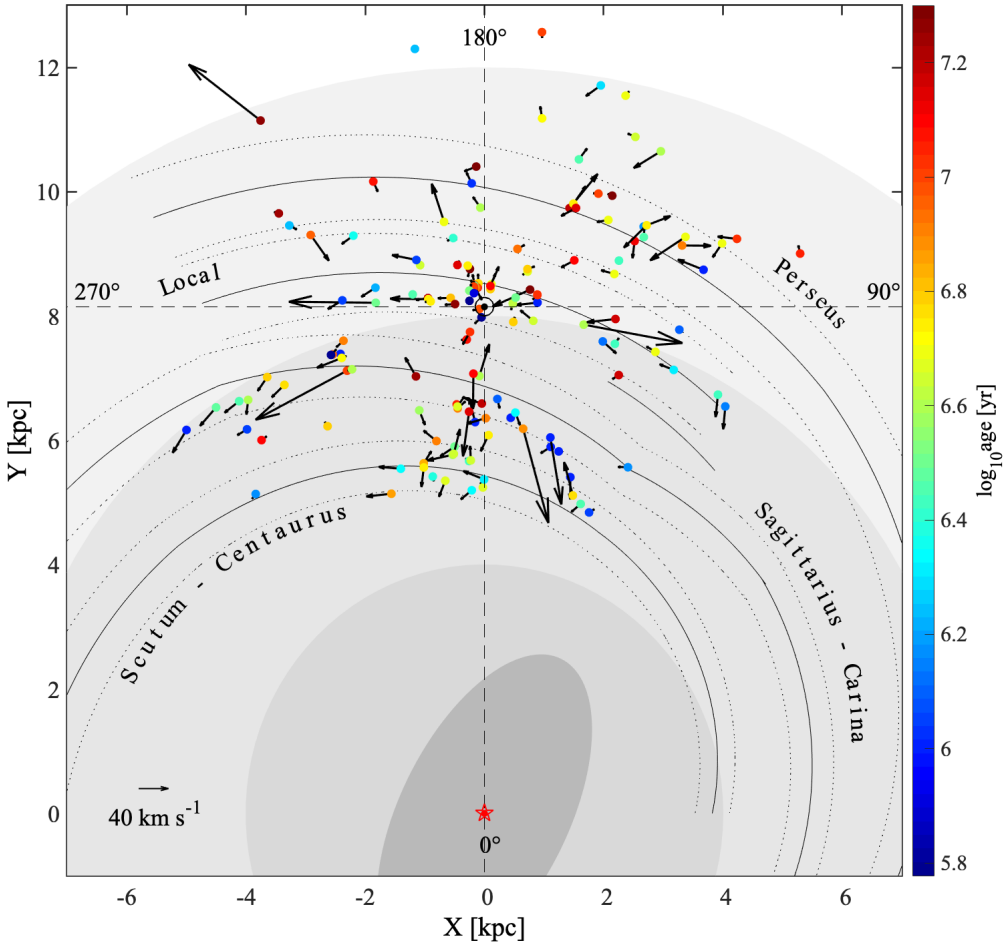

Fig. 2. Proper motion vectors of the YOCs. A motion scale of 40 km s^{-1} is indicated in the bottom left corner of the plot. The ages of OCs are colour coded. The background is the same as that of Reid et al. (2019).

masers (Reid et al. 2019) and OB stars (Xu et al. 2018b). We also find that the average lagging motion tends to increase as the OCs age (Fig. 3).

As discussed in Sect. 3.1, the YOCs gradually migrate away from their birth arms. With the kinematic data, the mean time for the YOCs to traverse their natal spiral arms could be estimated. The average arm width w is taken as 0.31 kpc, which is the mean width of the segments of the Perseus, Local, and Sagittarius-Carina Arms (Reid et al. 2019). We select the YOCs that are located in spiral arms according to the best-fit model of

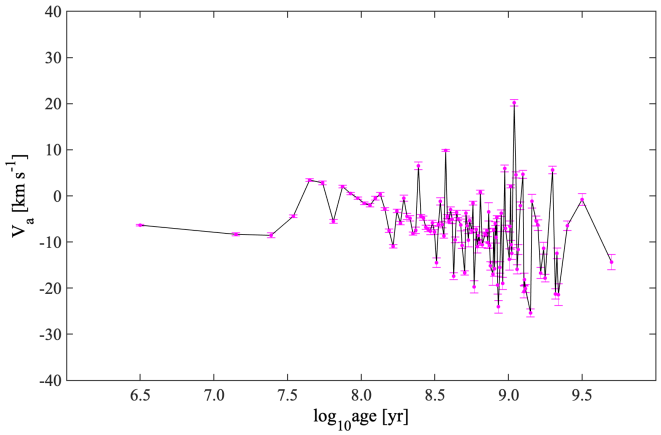

Fig. 3. Average peculiar motions of the OCs in the direction of Galactic rotation as a function of cluster age. The age bin is 5 Myr. The magenta symbols and error bars indicate the average PMs and their associated errors.

Reid et al. (2019), which is consistent with our fitting results with YOCs as shown in Fig. 1 and Table 2. As shown in Fig. 2, the YOCs approximately migrate either towards the Galactic centre direction or Galactic anti-centre direction. Hence, the travel speed of YOCs is defined as the average of the absolute values of the derived mean velocities. The travel velocity for the YOCs located in spiral arms, v, is estimated to be $14.6 \pm 0.2\,\mathrm{km\,s^{-1}}$. The mean time taken by a YOC to leave its natal spiral arms is simply estimated as $t = w \div v = 20.8 \pm 2.2$ Myr.

3.3. Scale height of OCs

In this section, we focus on the vertical distribution of OCs. The high-accuracy subsample with 3611 OCs (Sect. 2) is adopted. Statistically, about 43.4% of the 3611 OCs in our sample are located above the International Astronomical Union (IAU) defined Galactic plane ($b = 0°$). In previous works, asymmetric vertical distributions of gas or stars above and below the IAU-defined Galactic plane were commonly found (e.g., Anderson et al. 2019; Reid et al. 2019), which are generally interpreted as the Sun slightly deviating from the Galactic midplane towards the north Galactic pole, that is, the height of the Sun $z_\odot > 0$ pc. Many efforts have been made to determine the value of $z_\odot$ (e.g., Cantat-Gaudin et al. 2020, and references therein). By using the OCs with accurate *Gaia* parallaxes, we can refine the Galactic plane. We divide a subsample of 3376 OCs within 4.0 kpc of the Sun into 32 groups according to the OC ages, which are used to determine $z_\odot$. Then, the $z_\odot$ values of the 32 groups are averaged to obtain the mean vertical displacement of the Sun with respect to the Galactic plane. Here, the values of $z_\odot$ and the scale height are determined using the following function (Maíz-Apellániz 2001):

$$N(z) = N \times \exp\left[-\frac{1}{2}\left(\frac{z - z_\odot}{h}\right)^2\right], \quad (2)$$

where N is the central space density of OCs at $z = z_\odot$ with respect to the Galactic plane ($b = 0°$) and h is the scale height. By analysing the vertical distribution of OCs with the accurate *Gaia* parallaxes, the value of $z_\odot$ is refined to be 17.5 ± 3.8 pc above the true Galactic plane. This value is consistent with the results given by Buckner & Froebrich (2014) and Karim & Mamajek (2017), but smaller than that of Cantat-Gaudin et al. (2020). The value of $z_\odot = 17.5 \pm 3.8$ pc is adopted in this work to adjust the z-offsets of the OCs and calculate the scale heights.

Figure 4 shows the evolution of the scale height with cluster age for the 3376 OCs within 4.0 kpc of the Sun, which is consistent with the dispersion of the projected OCs as time goes by. The scale height is about 42 pc for the OCs with a mean age of $t_{\rm OC} \sim 1.5$ Myr and increases to about 130 pc for the OCs with $t_{\rm OC} \sim 850$ Myr. For the OCs with ages greater than $t_{\rm OC} \sim 1$ Gyr, the scale heights increase obviously. For the YOCs (ages < 20 Myr), the scale height is estimated to be 70.5 ± 2.3 pc. While for the OCs with ages of 20−100 Myr, the value is 87.4 ± 3.6 pc. The deviations of the scale heights of the very young OCs from those of HMSFR masers (19 ± 2 pc; Reid et al. 2019) and O−B_5 stars (34 ± 3 pc; Maíz-Apellániz 2001) are small, but increases gradually as OC age. These results are consistent with the properties discussed in Sect. 3.1. The OCs within an age of a few million years are still located in or very close to their birthplaces, hence have a small scale height. The spiral structure traced by these OCs resembles that of HMSFR masers or OB stars. But as the OCs age, the OCs gradually migrated further from their birthplaces and have larger scale height.

3.4. Regression analysis

Based on multiwavelength observations, we have some knowledge about the spiral structure of our Milky Way (e.g., Xu et al. 2018b). However, the lifetime of the spiral arms of the Galaxy of the galaxy is still a puzzle; the question is whether they are long-lived or short-lived. Many of the older OCs (ages > 20 Myr) in our sample have accurate parallaxes, proper motions, and radial velocities. With an appropriate model, we may trace their trajectories back tens of millions of years ago, until they were very young (i.e., ages < 20 Myr), and resided in their natal spiral arms in the past. With this method, the spiral structure in the past could be explored and compared with its current view. Such an approach provides a good and special way to inspect the evolutionary history of nearby spiral pattern and helps to address questions such as whether the spiral arms remain stable or have they evolved with time. Actually, tracing OCs back to their birthplaces has been proposed by some previous works (e.g., Dias & Lépine 2005; Dias et al. 2019) and used to determine the pattern speed of the Galaxy by assuming a stable spiral pattern. In the following, we adopt a regression analysis method to inspect the stability of nearby spiral structure.

Since the YOCs (<20 Myr) can well trace the spiral arms, we perform the regression analysis using 20-Myr intervals. The OCs in the age ranges of 20−40 Myr, 40−60 Myr, 60−80 Myr, and 80−100 Myr are regressed to 20, 40, 60, and 80 million years ago, respectively, by adopting a commonly used model of OC motions in the Milky Way (Wu et al. 2009). This model has been widely used to calculate the orbits of different objects (e.g., Odenkirchen et al. 1997; Allen et al. 2006), which employs an axisymmetric Galactic gravitational potential (Allen & Santillan 1991), consists of a spherical central bulge and a disc, plus a massive, spherical halo extending to a distance of 100 kpc from the Galactic centre (Paczynski 1990; Flynn et al. 1996). The total mass of the model is $9.0 \times 10^{11}\,M_\odot$, and the local total mass density in the solar neighbourhood is $0.15\,M_\odot\,\mathrm{pc}^{-3}$. The results of regression are shown in Fig. 5. We also fit spiral arms to the distributions of regressed OCs with the same method described in Sect. 3.1. The fitting results are listed in Table 3.

At present, about 72% of the YOCs are located in the spiral arms defined by HMSFR masers. In comparison, the

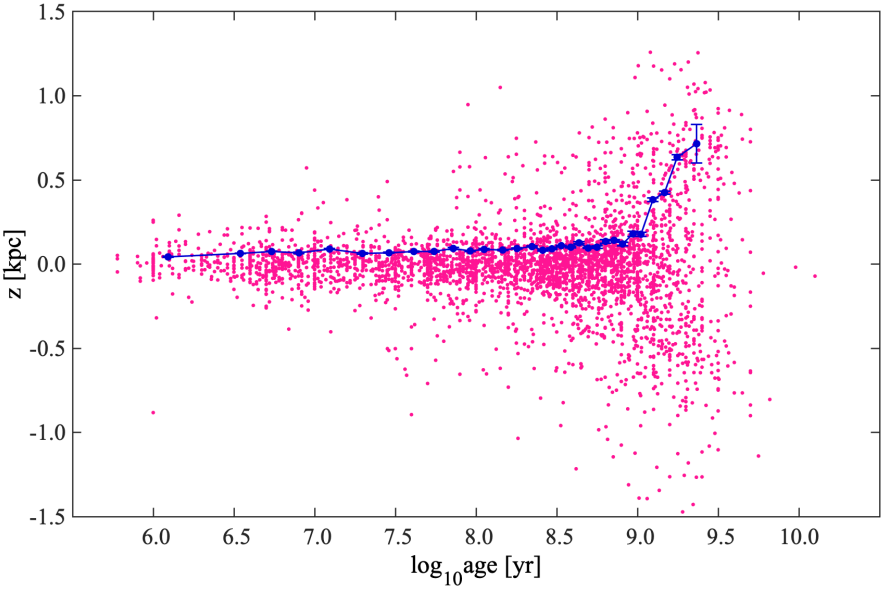

Fig. 4. Evolution of the scale height of OCs with OC age. The 3376 OCs within 4.0 kpc of the Sun are divided into 32 bins according to their ages. The blue line indicates the evolution of the scale height with cluster age. The blue dots correspond to the typical values of $\log_{10}$(age) in each bin. The solid magenta dots show the distances of the OCs to the Galactic plane as a function of cluster age.

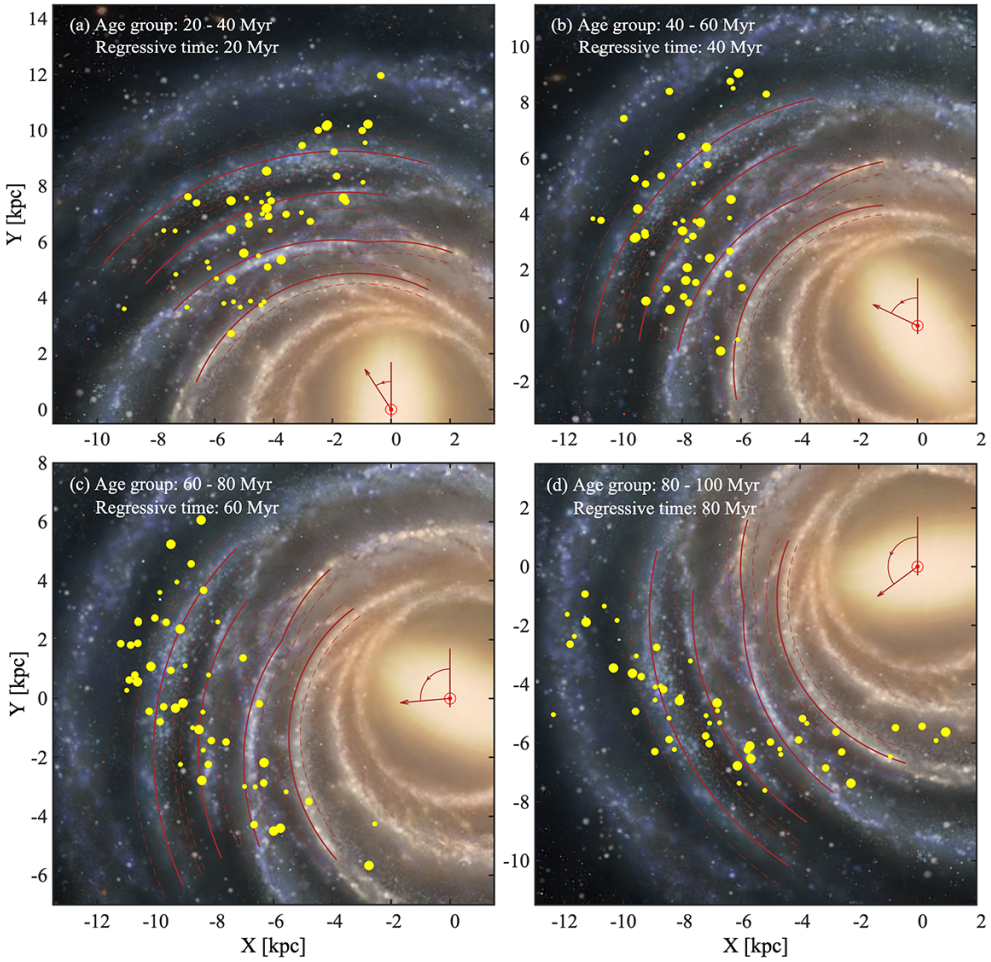

Fig. 5. Distributions of the regressed OCs. The OC ages have been grouped into: (*a*) 20−40 Myr, (*b*) 40−60 Myr, (*c*) 60−80 Myr, (*d*) 80−100 Myr, and traced back to 20, 40, 60, and 80 million years ago, respectively. The solid curved lines trace the centres (and dotted lines the widths enclosing 90% of the masers) of the best-fit spiral arms given by Reid et al. (2019), and have been rigidly rotated back to the past for comparison. The background is a new concept map of the Milky Way (credited by: Xing-Wu Zheng & Mark Reid BeSSeL/NJU/CFA), which is also rigidly rotated back to the past. The adopted pattern speed is 27 km s^{-1} kpc^{-1}.

Table 3. Best-fit results of the spiral arm parameters for the present-day OCs and the regressed OCs.

Age groups Regress to:	0–20 Myr	20–40 Myr 20 MYA	40–60 Myr 40 MYA	60–80 Myr 60 MYA	80–100 Myr 80 MYA
			Pitch angle: φ (degree)		
Sgr–Car Arm	16.2 ± 0.4	16.3 ± 1.0	16.2 ± 1.1	16.2 ± 1.0	16.0 ± 1.0
Local Arm	10.8 ± 0.6	10.8 ± 0.9	10.5 ± 1.0	10.5 ± 0.9	10.6 ± 1.0
Perseus Arm	9.6 ± 0.8	9.3 ± 0.9	9.5 ± 0.9	9.6 ± 0.9	9.5 ± 1.0
			Arm width: w (kpc)		
Sgr–Car Arm	0.27 ± 0.02	0.24 ± 0.09	0.24 ± 0.09	0.25 ± 0.09	0.25 ± 0.10
Local Arm	0.24 ± 0.06	0.28 ± 0.03	0.20 ± 0.05	0.23 ± 0.10	0.22 ± 0.09
Perseus Arm	0.33 ± 0.03	0.29 ± 0.09	0.29 ± 0.09	0.30 ± 0.10	0.31 ± 0.10

Notes. For each of the spiral arms near the Sun, we list its best-fit pitch angle (φ) and arm width (w), including their 1σ errors. Sgr–Car: Sagittarius-Carina Arm; MYA: million years ago.

percentages are about 39%–59% for the older clusters in the four different age groups (20–40 Myr, 40–60 Myr, 60–80 Myr and 80–100 Myr). After regression, many OCs are traced back to spiral arms in the past as shown in Fig. 5. We found that the percentages of regressed OCs in spiral arms increase to 71%–85%, which are comparable to the present-day value. The vertical scale height of the present-day OCs in the age groups of 20–100 Myr is about 87 pc. After regression, the scale height decreases to about 69 pc, close to the value for the present-day YOCs (~71 pc). In addition, we also notice that the best-fit pitch angles and arm widths of the Sagittarius-Carina, Local, and Perseus Arms at different regression times are consistent with each other within the uncertainties, which are all are very close to the present-day values traced by YOCs (Table 3). Hence, the spiral-arm features depicted by regressed OCs are roughly concordant with those traced by present-day YOCs. These results jointly suggest that the spiral arms near the Sun probably are compatible with a long-lived pattern, which has remained stable in the past 80 Myr. The Local Arm, which was thought to be a spur or branch but now is suggested as a major spiral arm segment, also has probably existed for a long time. However, although the spiral pattern can be roughly recognised over almost 80 Myr, it is not enough to support a long-lived stable pattern. It is also possible that the pattern could be in the last stages of disintegration. In the next works, we expect to further inspect this issue with more OCs and an improved model of OC motions in the Milky Way.

The evolutionary characteristics of nearby spiral arms revealed by OCs could provide some observational constraints on the formation mechanisms of the spiral arms of the Galaxy, which are hotly debated all along. There are two major competing scenarios: the dynamic spiral mechanism and the density wave theory. Proponents of the former argue that the spiral arms are short-lived, transient, and recurrent (Toomre & Toomre 1972; Sellwood & Carlberg 1984). Besides, the dynamic spiral mechanism may be able to explain the offsets in some local regions, but it does not predict the systematic positional offsets between spiral arms delineated by different kinds of tracers. Our above results are compatible with the long-lived and rigid, rotating nature of nearby spiral arms, and hence seem to conflict with the predictions of the dynamic spirals, indicating that this mechanism might be not prevalent for our Milky Way. In comparison, the (quasi-stationary) density wave theory suggests that the spiral arms are long-lived and rigidly rotated; this theory also predicts systematic spatial offsets between the spiral arms traced by HMSFRs and old stars (Lin & Shu 1964, 1966; Shu 2016). In this work we show that the evolutionary properties of spiral arms indicated by OCs are consistent with the expectations of the density wave theory. Besides, the results from the study addressing the metallicity gradient step near the Galactic corotation radius with OCs and cepheids also suggested long-lived spiral arms for the Milky Way (Lépine et al. 2003). However, we noticed that the density wave theory expects that the Milky Way has four major spiral arms and the Local Arm should not exist (Yuan 1969). The presence of the long-lived Local Arm ($\gtrsim$80 Myr) implied by our analysis enhances the challenge previously posed on this issue (Xu et al. 2013, 2016). Lépine et al. (2017) has interpreted the Local Arm as an outcome of the spiral corotation resonance, which traps arm tracers and the Sun inside it (also see Barros et al. 2021).

Density wave theory predicts that the Galactic spiral pattern should remain unchanged over a long time and rotate at a constant speed (Shu 2016). With the regression analysis method, we can constrain the spiral pattern speed by comparing the OC locations after regression with the positions of spiral arms rigidly rotated back to that time. Based on this, the present-day spiral arms are rotated back to 20, 40, 60, and 80 million years ago, respectively, and then compared with the distributions of the OCs after regression (Fig. 5). Under the assumption of a constant pattern speed, which is independent of the Galactocentric distance, the pattern speed is limited to be $26–28\,\mathrm{km\,s^{-1}\,kpc^{-1}}$, which is consistent with the values given by for example Dias & Lépine (2005), Dias et al. (2019), and Gerhard (2011). The results also suggest that the regression analysis method used in this work is feasible.

4. Conclusions

In summary, we have studied the evolution of the spiral arms of the Galaxy using a large catalogue of OCs based on *Gaia* EDR3. A regression analysis method applied to OCs indicates that the spiral arms near the Sun are compatible with a long-lived spiral pattern, which might have been essentially stable for at least the past 80 million years. In particular, the Local Arm is also probably long-lived in nature, and well traced by many YOCs, HMSFR masers, and OB stars, all of which suggest that the Local Arm is probable a major arm segment of the Milky Way. These evolutionary characteristics of spiral arms are more consistent with the expectations of the density wave theory. The dynamic spiral mechanism might be not prevalent for the Milky Way. These results are expected to be confirmed by conducting further studies with more OCs in the Milky Way.

Acknowledgements. We appreciate the anonymous referee for the instructive comments which help us a lot to improve the paper. This work was funded by the NSFC, grant numbers 11933011, 11873019, 11673066, 11988101 and by the Key Laboratory for Radio Astronomy. L. G. Hou thanks the support from the Youth Innovation Promotion Association CAS. We acknowledge Dr. Mark J. Reid for allowing us to use his program, utilised to fit the pitch angles of the Galactic spiral arms. We used data from the European Space Agency mission *Gaia* (http://www.cosmos.esa.int/gaia), processed by the *Gaia* Data Processing and Analysis Consortium (DPAC; see http://www.cosmos.esa.int/web/gaia/dpac/consortium). Funding for DPAC has been provided by national institutions, in particular the institutions participating in the *Gaia* Multilateral Agreement.

References

Allen, C., & Santillan, A. 1991, Rev. Mex. Astron. Astrofis., 22, 255
Allen, C., Moreno, E., & Pichardo, B. 2006, New. Astron., 652, 1150
Anderson, L. D., Wenger, T. V., Armentrout, W. P., et al. 2019, ApJ, 871, 145
Barros, D. A., Pérez-Villegas, A., Michtchenko, T. A., et al. 2021, Front. Astron. Space Sci., 8, 48
Becker, W. 1963, Z. Astrophys., 57, 117
Becker, W. 1964, in The Galaxy and the Magellanic Clouds, ed. F. J. Kerr, IAU Symp., 20, 16
Becker, W., & Fenkart, R. B. 1970, in The Spiral Structure of Our Galaxy, eds. W. Becker, & G. I. Kontopoulos, IAU Symp., 38, 205
Bobylev, V. V., & Bajkova, A. T. 2014, MNRAS, 437, 1549
Buckner, A. S. M., & Froebrich, D. 2014, MNRAS, 444, 290
Cantat-Gaudin, T., & Anders, F. 2020, A&A, 633, A99
Cantat-Gaudin, T., Jordi, C., Vallenari, A., et al. 2018, A&A, 618, A93
Cantat-Gaudin, T., Krone-Martins, A., Sedaghat, N., et al. 2019, A&A, 624, A126
Cantat-Gaudin, T., Anders, F., Castro-Ginard, A., et al. 2020, A&A, 640, A1
Camargo, D., Bica, E., & Bonatto, C. 2013, MNRAS, 432, 3349
Castro-Ginard, A., Jordi, C., Luri, X., et al. 2018, A&A, 618, A59
Castro-Ginard, A., Jordi, C., Luri, X., Cantat-Gaudin, T., & Balaguer-Nunez, L. 2019, A&A, 627, A35
Castro-Ginard, A., Jordi, C., Luri, X., et al. 2020, A&A, 635, A45
Dias, W. S., & Lépine, J. R. D. 2005, A&A, 629, 825
Dias, W. S., Alessi, B. S., Moitinho, A., & Lépine, J. R. D. 2002, A&A, 389, 871
Dias, W. S., Monteiro, H., Caetano, T. C., et al. 2014, A&A, 564, A79
Dias, W. S., Moitinho, A., Lépine, J. R. D., & Barros, D. A. 2019, MNRAS, 486, 5726
Fenkart, R. P., & Binggeli, B. 1979, A&AS, 35, 271
Ferreira, A. F., Corradi, W. J. B., Maia, F. F. S., Angelo, M. S., & Santos, J. F. C. 2020, MNRAS, 496, 2021
Flynn, C., Sommer-Larsen, J., & Christensen, P. R. 1996, MNRAS, 281, 1047
Gaia Collaboration (Prusti, T., et al.) 2016, A&A, 595, A1
Gaia Collaboration (Brown, A. G. A., et al.) 2018, A&A, 616, A1
Gaia Collaboration (Brown, A. G. A., et al.) 2021, A&A, 649, A1
Georgelin, Y. M., & Georgelin, Y. P. 1976, A&A, 49, 57
Gerhard, O. 2011, Mem. Soc. Astron. It. Suppl., 18, 185
Hao, C. J., Xu, Y., Wu, Z. Y., et al. 2020, PASP, 132, 034502
He, Z. H., Xu, Y., Hao, C. J., Wu, Z. Y., & Li, J. J. 2021, Res. Astron. Astrophys., 21, 093
Hou, L. G., & Han, J. L. 2014, A&A, 569, A125
Hou, L. G., & Han, J. L. 2015, MNRAS, 454, 626
Hubble, E. P. 1926, ApJ, 63, 236
Janes, K., & Adler, D. 1982, ApJS, 49, 425
Karim, M. T., & Mamajek, E. E. 2017, MNRAS, 465, 472
Kharchenko, N. V., Piskunov, A. E., Schilbach, E., et al. 2013, A&A, 558, A53
Lépine, J. R. D., Mishurov, Y., & Acharova, I. A. 2003, Boletim da Sociedade Astronômica Brasileira, 23, 28
Lépine, J. R. D., Michtchenko, T. A., Barros, D. A., et al. 2017, ApJ, 843, 48
Lin, C. C., & Shu, F. H. 1964, ApJ, 140, 646
Lin, C. C., & Shu, F. H. 1966, Proc. Natl. Acad. Sci., 55, 226
Lindblad, B. 1927, MNRAS, 87, 420
Liu, L., & Pang, X. 2019, ApJS, 245, 32
Lynga, G. 1982, A&A, 109, 213
Maíz-Apellániz, A. 2001, ApJ, 121, 2737
Moffat, A. F. J., Fitzgerald, M. P., & Jackson, P. D. 1979, A&AS, 38, 197
Moitinho, A. 2010, in Star Clusters: Basic Galactic Building Blocks Throughout Time and Space, eds. R. de Grijs, & J. R. D. Lépine, IAU Symp., 266, 106
Moitinho, A., Vázquez, R. A., Carraro, G., et al. 2006, MNRAS, 368, L77
Monteiro, H., Dias, W. S., Moitinho, A., et al. 2020, MNRAS, 499, 1874
Odenkirchen, M., Brosche, P., Geffert, M., & Geffert, H. J. 1997, New Astron., 2, 477
Oort, J. H., Kerr, F. J., & Westerhout, G. 1958, MNRAS, 118, 379
Paczynski, B. A. 1990, ApJ, 348, 485
Paladini, R., Davies, R. D., & De Zotti, G. 2004, MNRAS, 347, 237
Poggio, E., Drimmel, R., Cantat-Gaudin, T., et al. 2021, A&A, 651, A104
Reddy, A. B. S., Lambert, D. L., & Giridhar, S. 2016, MNRAS, 463, 4366
Reid, M. J., Menten, K. M., Zheng, X. W., et al. 2009, ApJ, 700, 137
Reid, M. J., Menten, K. M., Brunthaler, A., et al. 2014, ApJ, 783, 130
Reid, M. J., Menten, K. M., Brunthaler, A., et al. 2019, ApJ, 885, 131
Roeser, S., Demleitner, M., & Schilbach, E. 2010, AJ, 139, 2440
Russeil, D. 2003, A&A, 397, 133
Schmeja, S., Kharchenko, N. V., Piskunov, A. E., et al. 2014, A&A, 568, A51
Scholz, R.-D., Kharchenko, N. V., Piskunov, A. E., et al. 2015, A&A, 581, A39
Sellwood, J. A., & Carlberg, R. G. 1984, ApJ, 282, 61
Shu, F. H. 2016, ARA&A, 54, 667
Skrutskie, M. F., et al. 2006, AJ, 131, 1163
Soubiran, C., Cantat-Gaudin, T., Romero-Gómez, M., et al. 2018, A&A, 619, A155
Toomre, A., & Toomre, J. 1972, ApJ, 178, 623
Vázquez, R. A., May, J., Carraro, G., et al. 2008, ApJ, 672, 930
Wu, Z. Y., Zhou, X., Ma, J., & Du, C. H. 2009, MNRAS, 399, 2146
Xu, Y., Reid, M. J., Zheng, X. W., & Menten, K. M. 2006, Science, 311, 54
Xu, Y., Li, J. J., Reid, M. J., et al. 2013, ApJ, 769, 15
Xu, Y., Reid, M. J., Dame, T. M., et al. 2016, Sci. Adv., 2
Xu, Y., Bian, S. B., Reid, M. J., et al. 2018a, A&A, 616, L15
Xu, Y., Hou, L.-G., & Wu, Y.-W. 2018b, Res. Astron. Astrophys., 18, 146
Xu, Y., Hou, L. G., Bian, S. B., et al. 2021, A&A, 645, L8
Yuan, C. 1969, ApJ, 158, 871